19th Brazilian Congress of Thermal Sciences and Engineering
November 06th-10th, 2022, Bento Gonçalves - RS - Brazil

ENC-2022-0086
LINEAR STABILITY ANALYSIS OF CLOSURE MODELS FOR THE 1D TWO-FLUID MODEL: A FOCUS ON THE VELOCITY SHAPE FACTOR

Rodrigo L. F. Castello Branco
PUC-Rio: Departamento de Engenharia Mecânica , Rua Marquês de São Vicente 225, Gávea, Rio de Janeiro, RJ, 22541-900, Brazil
rcastello@puc-rio.br

João N. E. Carneiro
ISDB FlowTech, Av. Rio Branco 89, Centro - Rio de Janeiro, RJ, 20040-004, Brazil.
Joao.carneiro@isdbflowtech.com

Angela O. Nieckele
PUC-Rio: Departamento de Engenharia Mecânica , Rua Marquês de São Vicente 225, Gávea, Rio de Janeiro, RJ, 22541-900, Brazil
nieckele@puc-rio.br

Abstract. *The 1D Two-Fluid model is based on averaging processes to render the model tractable for industrial scale problems, resulting in information loss, which may render the standard model ill-posed. For vertical geometries, the model is unconditionally ill-posed, and closure relations play a key role, since they reintroduce missing physical parameters that may stabilize the flow and ensure well-posedness. The present work employs a new formulation for the liquid velocity shape factor C_L for vertical annular flows based on the local velocity distribution. A liquid film velocity profile model is devised and integrated to obtain the C_L formulation. Linear Stability Theory (LST) can be used to assess the hyperbolicity of a model by imposing small wavelength perturbations to the linearized version of the equation system and quantifying their growth. The novel model can be assessed in terms of its ability to induce damping of these disturbances. The viscous Kelvin-Helmholtz and the von Neumann stability analyses are performed to evaluate commonly employed closure models and the novel proposed formulation for the velocity shape factor. Results show that the novel model can guarantee well posedness of the linear system by introducing a growth rate plateau, blocking the unbounded growth of instabilities.*

Keywords: *1D Two-Fluid Model, Vertical Annular Flows, Momentum Flux Parameters, Stability Analysis, Assessment of closure models*

1. INTRODUCTION

Gas-liquid flows are important for several industries and are found in various processes such as refrigeration, steam power generation, boiling water nuclear reactors, and pipeline transport of oil and gas. In pipe flows, according to the spatial distribution of the gas and liquid phases, different flow patterns may occur, which are heavily influenced by the pipe geometry and phase flowrates. For vertical pipes with high gas flowrates, e.g., in natural gas production lines, annular flows may occur. When the slip velocities are high, waves may form in the gas-liquid interface, which can lead to the occurrence of phenomena such as liquid loading (Wang et al. 2022) and droplet entrainment (Rodrigues et al. 2020).

The one-dimensional Two-Fluid model is widely used for solving multiphase flows industrial problems. It solves a set of time and phase averaged conservation equations for each of the present phases, coupling them through interfacial transfer terms. The 1D model holds a reasonable trade-off between computational cost and accuracy and can predict complex phenomena associated with various flow configurations, such as the wave hydrodynamics in gas-liquid interfaces of annular flows. When employed with sufficiently fine meshes, the Two-Fluid model can capture interfacial instabilities in the numerical domain and their subsequent evolution into waves and slugs, opening the possibility to simulate the transition between different flow regimes using a single numerical framework. This relatively novel approach is referred to as Slug/Regime Capturing (Fullmer et al., 2014; Galleni and Issa, 2015; Nieckele and Carneiro, 2017; Fontalvo et al., 2020; Castello Branco et al., 2022).

Even though the 1D Two-Fluid model has gained widespread use in the industry, it still faces several challenges, especially regarding hyperbolicity. Due to the averaging processes, information about the flow field and momentum transfer is lost from the system of equations. As a result, the standard formulation is known to be conditionally well-posed for horizontal and inclined geometries and unconditionally ill-posed for vertical geometries. In an ill-posed scenario, the

high frequency instabilities captured by the numerical system are amplified at an unbounded rate, and eventually contaminate the physical solution. This process may render the results meaningless and will manifest as an inability to obtain a mesh convergent solution.

To ensure hyperbolicity, one can reinject information that was lost in the averaging processes through closure relations, which may also damp short wavelength perturbations. The development of accurate closure relations is an active challenge in one-dimensional modelling. Several formulations have been proposed for closure models such as the wall and interfacial friction factors (Wallis, 1969; Whalley and Hewitt, 1978; Belt et al. 2009; Aliyu et al., 2017), dynamic pressure models related to the phase velocities differences (Bestion, 1990; Fowler and Lisseter, 1992; Fontalvo et al., 2020), and momentum flux parameters due to the non-uniformity of the velocities at the cross section (Song and Ishii, 2000; Fontalvo et al., 2020; Castello Branco et al., 2022).

Linear stability theory (LST) is often employed to assess the dynamics of instabilities by analysing the characteristics of the system of equations. The stability analyses introduce infinitesimal perturbations into stable flow fields and quantify the growth or decay of these perturbations under a system of mathematical or discrete equations. The result is a dispersion relation that correlates the growth rates with a frequency or wavelength spectrum. In ill-posed systems, the growth rate will increase radically for critical frequencies/wavelengths.

Barnea and Taitel (1993) devised inviscid and viscous formulations for the Kelvin-Helmholtz instability applied to stratified flow. They produced a stability map for varying liquid and gas superficial velocities, showing the neutral-stability regions for both formulations, and how they intersect with flow pattern transition. Liao et al. (2008) performed a discrete stability analysis on a stratified configuration using the Two-Fluid model with three spatial discretization schemes. They assert that the instabilities due to ill-posedness trigger the unbounded growth of round-off errors, effectively rendering the physical solution useless. Galleni and Issa (2015) present the differential and discrete stability analyses to study the ill-posedness of slug flow in vertical pipes, which showed that the discretization of the equations introduces a cut-off limit to the growth of instabilities. Kushnir et al. (2017) assessed the introduction of closure relations and their influence on the stability of stratified flows. Castello Branco et al. (2022) evaluated, with discrete and differential LST approaches, different closure parameters, including the liquid shape factor. The results obtained have improved the understanding of the liquid momentum flux parameter behavior in numerical simulations. They suggested, in agreement with Fontalvo et al. (2020), that the hypothesis of a constant value should be assessed further.

The present work aims to expand on previous studies by introducing a locally varying formulation for the liquid momentum flux parameter. A velocity profile model, which depends on the local flow quantities, is devised, and integrated to obtain a pre-integrated model for C_L. Linear stability analyses are carried out to evaluate the extent to which the novel formulation can damp the growth of spurious instabilities and bring about well-posedness to the system. A viscous approach of the Kelvin-Helmholtz analysis and a discrete von Neumann analysis are carried out.

2. MODELING

The Two-Fluid Model (Ishii and Hibiki, 2011) is employed in the present work to solve a two-phase annular flow. It consists of a set of time and phase averaged conservation equations for each phase. The interactions between the phases are treated through the interfacial terms in each balance equation. The 1D formulation consists of an area average in the pipeline cross section A. For vertical isothermal flows, the balance equations for phase ℓ (G for gas and L for liquid) are

$$\frac{\partial\, \rho_\ell\, \alpha_\ell}{\partial\, t} + \frac{\partial\, \rho_\ell\, \alpha_\ell U_\ell}{\partial\, x} = 0 \tag{1}$$

$$\frac{\partial\, (\rho_\ell\, \alpha_\ell\, U_\ell)}{\partial\, t} + \frac{\partial\, (\rho_\ell\, \alpha_\ell\, C_\ell\, U_\ell^2)}{\partial\, x} = -\alpha_\ell\, \frac{\partial\, P_{\ell_i}}{\partial\, x} - \frac{\partial \alpha_\ell \left(P_\ell - P_{\ell_i}\right)}{\partial x} - \alpha_\ell\, \rho_\ell\, g - \frac{\tau_{w\ell}\, S_\ell}{A} \pm \frac{\tau_i\, S_i}{A} \tag{2}$$

where t and x represent the time and axial coordinate, respectively. ρ_ℓ and U_ℓ are the density and average phase velocity. α_ℓ is the volume fraction, which is defined as

$$\alpha_\ell = \frac{\forall_\ell}{\forall} \qquad ; \qquad \sum_\ell \alpha_\ell = 1 \tag{3}$$

$\forall_\ell$ is the volume occupied by phase ℓ and $\forall$ is the total volume. C_ℓ is the momentum flux parameter for phase ℓ, P_ℓ and P_{ℓ_i} are the phase average pressure and their corresponding values at the interface, respectively. g is the gravity acceleration, $\tau_{w\ell}$ and τ_i are the wall-phase and interfacial shear stresses, S_ℓ is the wetted perimeter. For annular flows, the liquid film wetted perimeter is defined $S_L = \pi D$, there is no gas wetted perimeter ($S_G = 0$) and the interface perimeter is equal to $S_i = \pi(D - 2\, h_L)$, where the liquid film thickness is $h_L = D/2\, \left(1 - \sqrt{\alpha_G}\right)$ and D is the pipe diameter, with cross section area, $A = \pi\, D^2/4$.

Due to the averaging process of the 1D Two-Fluid Model, several parameters must be defined/modeled to close the one-dimensional system of equations and compensate for the loss of information. These parameters are referred to as closure relations and are defined in the next sub-section.

2.1 Closure relations

The wall/liquid and interfacial shear stress are defined in terms of a Fanning friction factor as

$$\tau_{wL} = \frac{1}{2}\, f_L\, \rho_L \mid U_L \mid U_L \quad ; \quad \tau_i = \frac{1}{2}\, f_i\, \rho_G \mid U_G - U_L \mid (U_G - U_L) \tag{4}$$

In the present work, the correlations selected for the friction factors are Kosky and Staub (1971) and Whalley and Hewitt (1978) for the wall/liquid (f_L) and interfacial (f_i) friction factors, respectively.

$$f_L = \begin{cases} \dfrac{16}{Re_{sL}} & if \quad Re_{sL} < 50 \\ \dfrac{12.7937}{Re_{sL}^{0.9428}} & if\ 50 \leq Re_{sL} \leq 1483 \\ \dfrac{0.081}{Re_{sL}^{0.25}} & if \quad Re_{sL} > 1483 \end{cases} \qquad f_i = \frac{0.079}{Re_{sG}^{0.25}} \left[1 + 12 \left(\frac{\rho_L}{\rho_G}\right)^{1/3} \left(1 - \sqrt{\alpha_G}\right)\right] \tag{5}$$

Further, the difference between the bulk pressure and its corresponding value at the interface is modelled as a dynamic pressure term ΔP_{dyn_ℓ} based on the bulk and interface relative velocity, defined below

$$\Delta P_{dyn_\ell} = P_\ell - P_{\ell_i} = W_{f\ell}\, \rho_{ref} (U_L - U_i)^2 \tag{6}$$

where $W_{f\ell}$ is an empirical parameter, ρ_{ref} is a reference density, and U_i is the interface velocity. In the present work, three dynamic pressure models are evaluated and are presented in Table 1.

Table 1. Dynamic pressure models

Model	W_{fG}	W_{fL}	ρ_{ref}	U_i
ΔP_{dyn_I}(Fowler & Lisseter, 1992)	0	0.02	ρ_L	$2\, U_L$
$\Delta P_{dyn_{II}}$ Bestion, 1990)	1.2	1.2	$\rho_m = \dfrac{\alpha_L\, \alpha_G\, \rho_G\, \rho_L}{\alpha_G\ \rho_L + \alpha_L\, \rho_G}$	U_G
$\Delta P_{dyn_{III}}$ (Fontalvo et al., 2020)	0	0.02	ρ_L	$U_{wave} = \dfrac{\sqrt{\rho_G}\, U_{sG} + \sqrt{\rho_L}\, U_{sL}}{\sqrt{\rho_G} + \sqrt{\rho_L}}\ \dfrac{50\, Re_{sL}^{0.16}}{Re_{sG}^{0.38}\, ST_w^{0.13}}$

Model $\Delta P_{dyn_{III}}$ depends on the gas and liquid superficial Reynolds, $Re_{s\ell}$; $U_{s\ell} = \alpha_\ell\, U_\ell$; a surface tension factor ST_w and viscosity number; where ST_w, given by

$$Re_{s\ell} = \frac{\rho_\ell U_{s\,\ell} D}{\mu_\ell} \quad ; \quad ST_w = \begin{cases} 0.25 \ if\ N_\mu > 1/15 \\ 0.028/N_\mu{}^{0.8} \quad if\ N_\mu \leq 1/15 \end{cases} \quad ; \quad N_\mu = \frac{\mu_L}{\sqrt{\rho_L\, \sigma \left[\frac{\sigma}{g\,(\rho_L - \rho_G)}\right]^{0.5}}} \tag{7}$$

The interfacial pressure term in the momentum equations accounts for the pressure jump over the interface due to surface tension, and is defined by the Young-Laplace equation,

$$P_{Gi} - P_{Li} = \sigma\, \kappa \quad \text{where} \quad \kappa = \kappa_1 + \kappa_2 \quad ; \quad \kappa_1 = \frac{\partial^2 h_L}{\partial x^2} = \left(\frac{D}{4}\frac{1}{\sqrt{\alpha_G}}\right)\frac{\partial^2 \alpha_L}{\partial x^2} + \left(\frac{D}{8}\frac{1}{\alpha_G^{3/2}}\right)\left(\frac{\partial \alpha_L}{\partial x}\right)^2 \quad ; \quad \kappa_2 = \frac{2}{D - 2h_L} = \frac{2}{D\sqrt{\alpha_G}} \tag{8}$$

where σ and κ are the surface tension coefficient and curvatures in the axial and transversal directions.

2.2 Momentum flux parameter

The multiplying parameter C_ℓ in the convective term in the LHS of the momentum equations (Eq. 2) aims to restore information regarding the non-uniformity of velocity profile in the cross section. In the standard Two-Fluid Model, the averaging process removes information regarding the velocity distribution in the cross-section, which is akin to assuming that the profile is completely flat for both phases. The shape factor is defined as

$$C_\ell = \frac{(1/A_\ell) \int_{A_\ell} u_\ell^2\, dA_\ell}{\left[(1/A_\ell) \int_{A_\ell} u_\ell\, dA_\ell\right]^2} \tag{9}$$

Depending on the flow, the velocity profile is different, consequently C_ℓ is also different. For example, according to Inada et al. (2004), for high gas velocities, the velocity profile of the liquid film can be approximated as linear (i.e., Couette flow), which results in a C_L = 1.33 value. A parabolic profile results in a C_L value of 1.20. For a turbulent velocity

profile, the 1/7 power-law formulation renders a shape factor of C_L = 1.02. Fontalvo et al. (2020) have tested the common C_L values of 1.00, 1.05, 1.20 and 1.33 coupled with other closure models and observed that the C_L = 1.05 with a dynamic pressure model yielded the best agreement with experimental data.

Recent studies have employed pre-integrated models for locally defined momentum flux parameter from analytical velocity profiles. This has not yet been sufficiently explored for annular flows. In the present work, we aim to devise a velocity profile model for the annular liquid film to yield an instantaneous pre-integrated formulation for C_L. The coordinate system for the velocity profile integration is shown in Fig. 1.

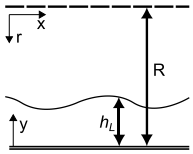

Figure 1. Coordinate system for the liquid film velocity profile integration.

To generalize the results, the following non-dimensional velocity, wall distance, radius, and liquid film thickness are employed

$$u^+ = \frac{U_L}{u_\tau} \quad ; \quad y^+ = y\frac{u_\tau}{\nu_L} \quad ; \quad R^+ = \frac{R\,u_\tau}{\nu_L} \quad ; \quad h_L^+ = \frac{h_L u_\tau}{\nu_L} \tag{10}$$

These non-dimensional quantities are written in terms of the friction velocity u_τ and kinematic viscosity ν_L. Re_τ is the friction velocity Reynolds number defined as

$$Re_\tau = \frac{u_\tau D_{hL}}{\nu_L} \quad ; \quad u_\tau = \sqrt{\frac{\tau_{wL}}{\rho_L}} \quad ; \quad \nu_L = \frac{\mu_L}{\rho_L} \quad ; \quad D_{hL} = \frac{4\,A_L}{S_L} = 4\,h_L\left(1 - \frac{h_L}{D}\right) \tag{11}$$

Employing the dimensionless variables, the liquid momentum flux parameter can be determined with

$$C_L = \frac{1}{8}\left(\frac{D}{D_{hL}}\right) Re_\tau^2 \, \frac{\int_0^{h_L^+} (u^+)^2 (R^+ - y^+)\,dy^+}{\left[\int_0^{h_L^+} u^+ (R^+ - y^+)\,dy^+\right]^2} \tag{12}$$

The liquid film velocity profile model devised in this work is a simplified version of the universal velocity profile for single phase flow (Dobran, 1983), with a viscous sublayer and a turbulent layer. The logarithmic profile of the turbulent layer is adjusted to couple the velocity distribution in the liquid film with the gas core region through the interfacial shear stress, which is consistent with the Two-Fluid formulation. The proposed velocity profile is defined as

$$\begin{cases} u^+ = y^+ & , \quad 0 \le y^+ \le y_{sub}^+ \\ u^+ = a \ln y^+ + b & , \quad y_{sub}^+ < y^+ \le h_L^+ \end{cases} \tag{13}$$

$$a = \frac{\tau_i^+}{0.14} \quad ; \quad b = y_{sub}^+ - \frac{\tau_i^+}{0.14} \ln y_{sub}^+ \quad ; \quad \tau_i^+ = \frac{\tau_i}{\rho_L u_\tau^2} \quad ; \quad y_{sub}^+ = 5 \quad ; \quad y_{up}^+ = 30 \tag{14}$$

The procedure to obtain the momentum flux parameter values from the local flow quantities is described below.

i. Obtain the liquid and gas phase velocities.

ii. Obtain or calculate the liquid film thickness h_L, either from simulation results or from an equilibrium estimate.

iii. Calculate the wall and interfacial shear stresses and the non-dimensional liquid film height h_L^+.

iv. Determine C_L by integrating the proposed velocity profile in the range of $y^+ = [0 \;\; h_L^+]$

Figure 2 shows a C_L map obtained with the procedure described above, for a configuration of air/water flow with $D = 0.035$m. An equilibrium film height is estimated based on the superficial velocities, diameter, and fluid properties. A significant dependency on the liquid superficial velocity is observed, with a smaller dependency on the gas superficial velocity, particularly for lower U_{sG}. The low liquid superficial velocities yield higher relative phase velocities, which promotes a thinner liquid film configuration. The resulting velocity profile for thin films is approximately linear, therefore higher C_L values are obtained. As the liquid superficial velocity increases, the C_L value naturally increases as well.

In order to improve the efficiency of the model, a simplified formulation is proposed. From the data obtained in the map shown in Fig. 2, a clear dependency on the liquid velocity is observed. Thus, a power profile model is fitted into the data to extract this dependency. The formulation is outlined in Eq. (15).

$$\begin{cases} C_L = 1.33 & , \quad Re_L \le 303 \\ C_L = 1.37 Re_L^{-0.13} + 0.66 & , \quad Re_L > 303 \end{cases} \tag{15}$$

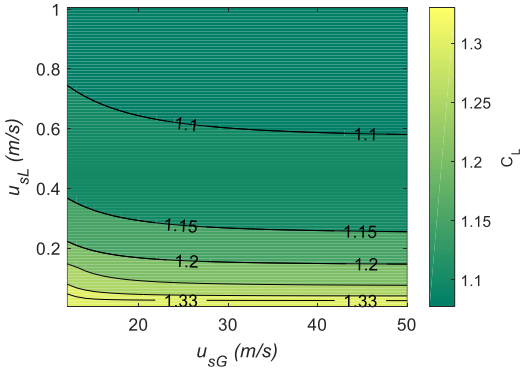

Figure 2. Map of liquid momentum flux parameter as a function of the gas and liquid superficial velocities.

2.3 Stability analysis

The linear stability analysis of the 1D Two-Fluid Model performed in this work is similar to the procedure described in Castello Branco et al. (2022), with the addition of the flow dependent momentum flux parameter formulation. Firstly, the momentum equations are combined to eliminate the pressure term. The unknown vector is thus given by $\boldsymbol{\varphi} = (\alpha_L, U_G, U_L)^T$. By perturbing the solution vector, we may decompose it in a base and disturbed portions $\boldsymbol{\varphi} = \bar{\boldsymbol{\varphi}} + \boldsymbol{\varphi}'$. The linearized perturbed system can be written as

$$\left(\overline{\boldsymbol{A}}\,\frac{\partial}{\partial t} + \overline{\boldsymbol{B}}\,\frac{\partial}{\partial x} - \widehat{\boldsymbol{D}}\right)\boldsymbol{\varphi}' = \mathbf{0} \tag{16}$$

The viscous Kelvin–Helmholtz (VKH) differential analysis can be applied to estimate the growth rate of disturbances of the mathematical system, while the von Neumann stability analysis evaluates the discrete differential equations. The perturbed quantity is defined for the differential and discrete approaches as

$$\varphi' = \varepsilon_\varphi\, e^{i(\omega\, t - kx)} \quad , \quad \varphi'_P = \varepsilon_\varphi\, E\, e^{i\phi} \tag{17}$$

where ε_φ is the amplitude, ω is the angular frequency, k is the wave number and $i = \sqrt{-1}$. $\phi = k\,\Delta x$ is the phase angle, and E is an amplitude factor. For both approaches, liquid and gas velocities are assumed positive, and the gas is approximated as incompressible. To take the variation of the shape factor in terms of the novel formulation into account, C_L has been written as a function of the void fraction α_L, liquid and gas velocities. The axial derivative of C_L is

$$\frac{\partial C_L}{\partial x} = \frac{\partial C_L}{\partial \alpha_L}\frac{\partial \alpha_L}{\partial x} + \frac{\partial C_L}{\partial U_L}\frac{\partial U_L}{\partial x} + \frac{\partial C}{\partial U_G}\frac{\partial U_G}{\partial x} \tag{18}$$

and, for the discrete analysis, the perturbed variable at the nodal point is

$$\hat{C}_{L_P} = \frac{\partial C_L}{\partial \alpha_L}\hat{\alpha}_{L_P} + \frac{\partial C_L}{\partial U_G}\widehat{U}_{G_P} + \frac{\partial C_L}{\partial U_L}\widehat{U}_{L_P} \tag{19}$$

The perturbed variable vector is introduced in Eq. (17), resulting in $\boldsymbol{M\varepsilon} = \mathbf{0}$. For the discrete analysis, a staggered grid was employed, and the conservation equations were discretized with TVD scheme (Versteeg and Malalasekera, 2007), based on the Van Leer limiter function: $\psi(r) = (r + |r|)\,/\,(1 + r)$, with $\psi(\hat{r}_\alpha) = 1$.

The characteristic roots of the system are obtained by taking the determinant of $\boldsymbol{M}$. Real roots correspond to a hyperbolic system, while complex roots correspond to an elliptic system, causing ill-posedness to the 1D Two-Fluid model, and any infinitesimal disturbance will cause the waves to grow exponentially without upper bound. For both differential and discrete system, a non-trivial solution for $\left(\varepsilon_{\alpha_L}, \varepsilon_{U_G}, \varepsilon_{U_L}\right)^T$ exists when the determinant of the system matrix $\boldsymbol{M}$ is zero. The dispersion relation Ω is defined as a second order polynomial

$$\alpha\,\Omega^2 + \beta\,\Omega + \gamma = 0 \tag{20}$$

in which, for the differential case, $\Omega = \omega$. The imaginary component of ω determines the temporal growth rate of the perturbation. For the discrete case, $\Omega = G^{-1}$, where G is the amplification factor, given by the ratio of perturbation amplitude at two consecutive time instants. The growth rate ω_i is calculated as (Galleni and Issa, 2015):

$$-\omega_i = \frac{(G-1)}{\Delta t} \quad ; \quad G = \frac{E^{n+1}}{E^n} \quad ; \quad t^{n+1} = t^n + \Delta\, t \tag{21}$$

where Δt is the time step. Amplification of disturbances occurs when $-\omega_i > 0$.

3. RESULTS AND DISCUSSION

To evaluate the impact of different combinations of closure models in the Two-Fluid model, through Linear Stability Analyses, for vertical annular, two configurations were selected, and their set-up are summarized in Table 2.

Table 2. Summary of the experimental set-ups selected for the stability analysis.

Configuration	Geometry		Gas			Liquid		
	Diam. D (mm)	Length L (m)	$Re_{sG} \times 10^{-4}$	Density (kg/m^3)	Viscosity (cP)	Re_{sL} $(-)$	Density (kg/m^3)	Viscosity (cP)
I - Kaji (2008)	19.0	6.87	4.14	1.75	0.0179	569	998.2	1.00
II - Zhao *et al.* (2013)	34.5	2.00	9.12	1.18	0.0179	603	998.2	1.00

Here, commonly used models for the dynamic pressure term and liquid momentum flux parameter are assessed in terms of their ability to stabilize the system of equations, through the optics of a differential and discrete stability analyses. The novel C_L model proposed in this work is also evaluated. In the discrete analysis, mesh spacings varying from $\Delta x/D$ = 1 to 0.015625 were selected, and the CFL number, defined as $CFL_G = U_G\,\Delta t/\Delta x$, is kept constant equal to 0.5.

3.1 Effect of the dynamic pressure

Figure 3 shows the dispersion curves for the case with no regularization (Fig.3a) and the selected ΔP_{dyn} models (Fig. 3b-d) for the II-Zhao case. For these tests, the shape factors were kept equal to one. The dispersion curves correlate the growth rate of the system with a frequency spectrum. The dashed curve in Fig. 3 is associated with the differential analysis, whereas the colored curves are associated with the different mesh refinements of the von Neumann analysis. We observe from Fig. 3 that the dynamic pressure models ΔP_{dyn_I} and $\Delta P_{dyn_{III}}$ had nearly no damping effect in the discrete curves and were unable to halt the unbounded wave growth as seen in the differential curves. The $\Delta P_{dyn_{II}}$ showed significant damping effects for finer meshes ($\Delta x/D$ = 0.03125 and 0.015625) and introduced a growth rate plateau at $-\omega_i = 35\ \mathrm{s}^{-1}$ for very high frequencies, which would characterize a well-posed unstable system. However, the grid refinement levels that would be required for mesh convergence to occur with this regularization mechanism are virtually unattainable. Additionally, for practical mesh sizes, no observable change in the discrete growth rate curves occurred.

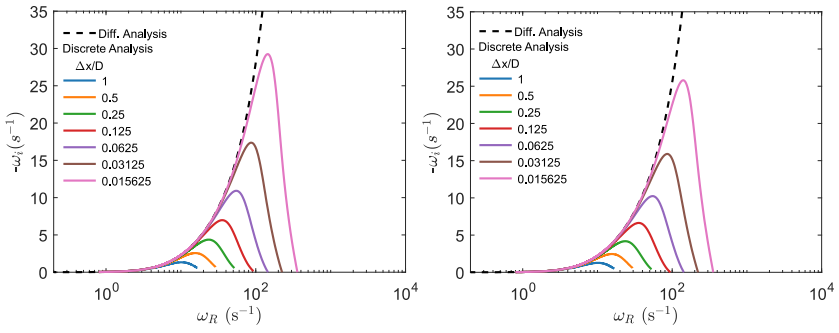

(a) No model ΔP_{dyn} (b) Model ΔP_{dyn_I}

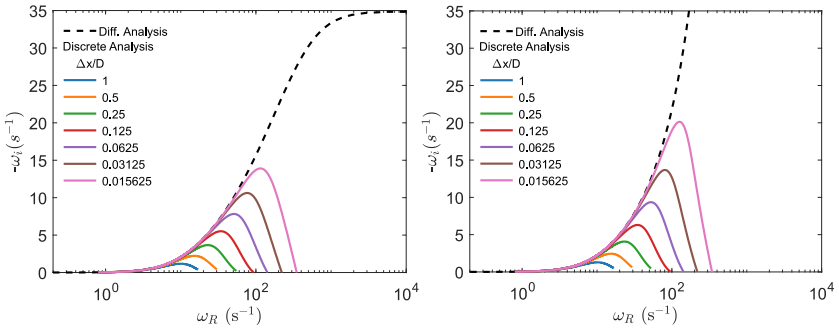

(c) Model $\Delta P_{dyn_{II}}$ (d) Model $\Delta P_{dyn_{III}}$

Figure 3. Influence of the dynamic pressure model in the growth rate. Case II-Zhao.

The small effect of the dynamic pressure model is influenced by the low value of the empirical constant W_{fL} in the formulation of models ΔP_{dyn_I} and $\Delta P_{dyn_{III}}$ ($W_{fL} = 0.02$; $W_{fG} = 0$). Thus, an evaluation of different W_{fL} values was carried out. Figure 4 shows effect of varying the W_{fL} constant with model $\Delta P_{dyn_{III}}$. Increasing its value, decreases the maximum growth rates in the discrete analysis. In fact, a small increase to a value of 0.05 renders the system well-posed, with a growth rate plateau of approximately $-\omega_i = 22\ \mathrm{s}^{-1}$. Raising the value to 0.5 virtually stabilizes all wavelengths. In this scenario, the system approaches a well-posed stable state, and wave formation does not occur. Careful consideration of the W_{fL} parameter must be performed in terms of its physical soundness.

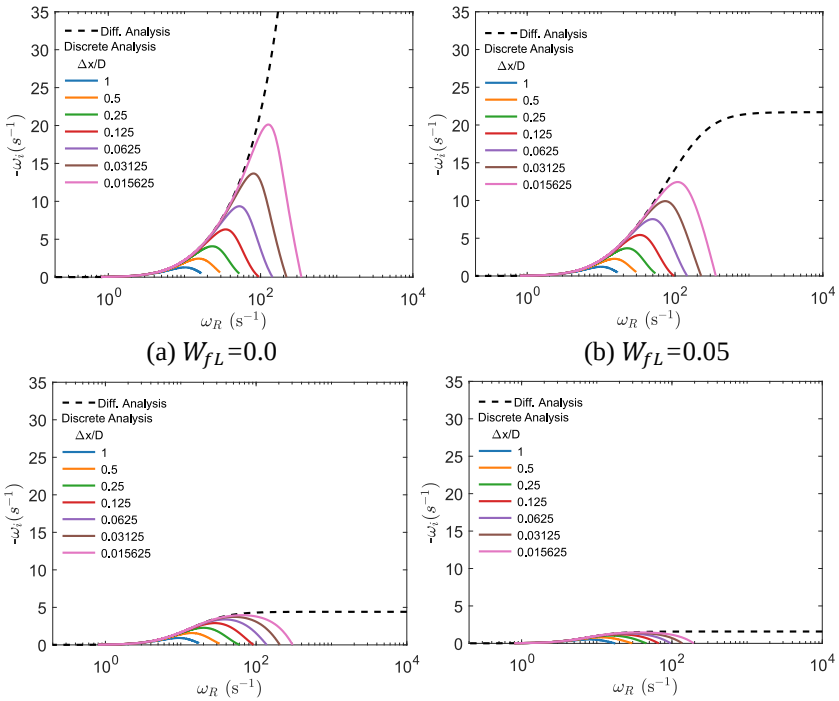

(a) W_{fL}=0.0 (b) W_{fL}=0.05

(c) W_{fL}=0.2 (d) W_{fL}=0.5

Figure 4. Influence of the empirical constant of the dynamic pressure model in the growth rate. Case II-Zhao.

3.2 Effect of the liquid momentum flux parameter

To analyze the impact of the shape factor in the disturbance's growth rate, no dynamic pressure model was included. Figure 5 depicts the influence of the momentum flux parameter values in the damping of perturbations for the I-Kaji case. A $C_L = 1.00$, i.e., shape factor for uniform velocity profile, clearly results in an ill-posed system. A small increase to $C_L = 1.05$ has a positive effect in damping the disturbances, as can be seen from the decrease in the peaks of the von Neumann curves. However, the effect was not significant enough to render the system well-posed. An increase to a constant $C_L = 1.20$ value introduces a plateau at a smaller growth rate and suggests that a mesh convergent solution can be attained. Thus, $C_L = 1.20$ can guarantee the hyperbolicity of the system. The novel proposed model is also able to guarantee the system's hyperbolicity, as the plateau occurs for very low growth rate values. C_L = 1.33 showed good stability properties, but arguably may over-stabilize the system, to the point where the disturbance waves in wavy annular flow become unphysically small.

From the results of C_L 1.33 and the proposed model, an important discussion pertaining to the physical fidelity on the damping effect of closure models arises. In light of this discussion, Fig. 6 shows numerical simulation results of film thickness spatial series for the II-Zhao case at $t = 100$s. All C_L values and the proposed model are tested. From the spatial evolution of the film, one can notice the high amplification of waves presented by C_L 1.00 and 1.05, which results in a very narrow liquid film distribution in between the waves. As the C_L value is raised to 1.20, the wave amplitudes decrease, and the film thickness increases. The highest C_L value, 1.33, yields very small waves.

The variable C_L model shows a very positive behavior: even though the stability analysis shows that its growth rate plateau is lower, closer to the results of C_L 1.33, it is able to amplify the waves such that the amplitudes are comparable to C_L 1.20. This occurs because the locally defined momentum flux parameter model can vary throughout the domain, which means that the amplification rate also varies, allowing the model to locally amplify or damp the system based on the physical behavior of the flow quantities. Figure 7 better illustrates the non-linear behavior of the variable shape factor model, where at the linear region, a nearly constant C_L value is obtained. The onset of waves prompts a significant C_L variation to account for the changes in the velocity profiles. For the liquid film in-between waves, which is considerably

narrower, the shape factor approximates 1.33. As the disturbance waves begin to form, the shape factor drops to lower values, reaching minima of about 1.15. These local variations are responsible for the wave behavior of Fig. 6, which is detected by the LST analysis.

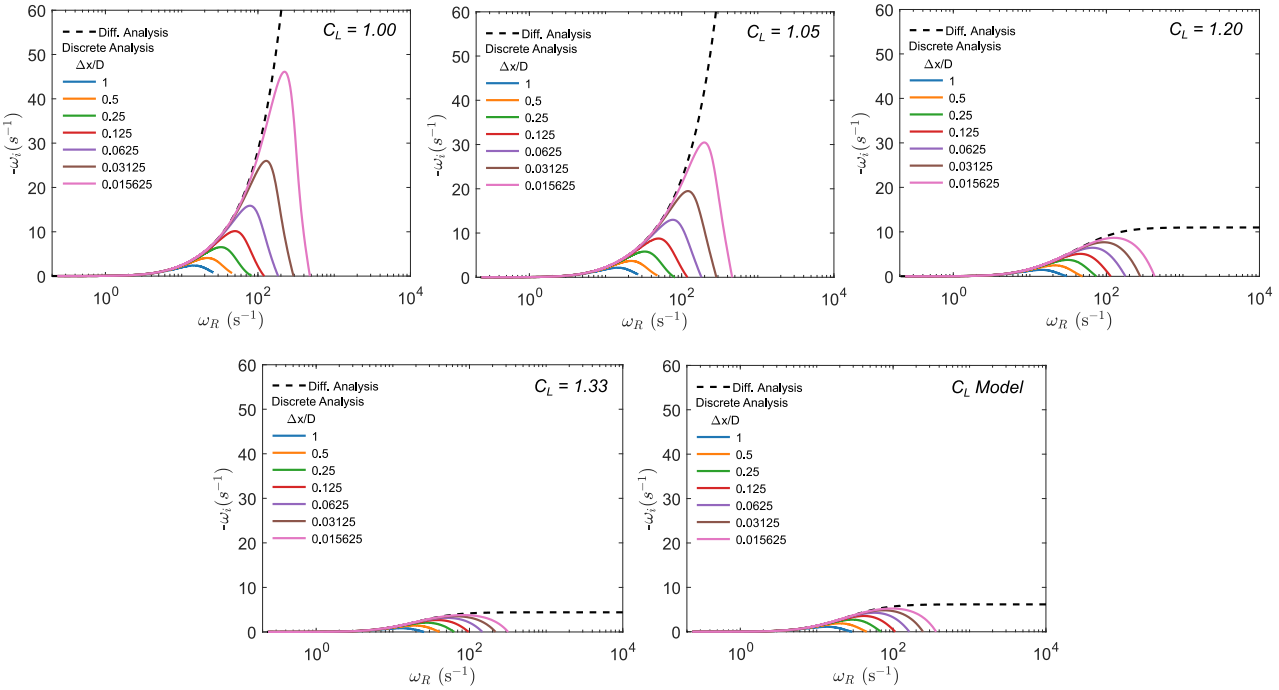

Figure 5. Influence of the momentum flux parameter in the growth rate. Case I-Kaji.

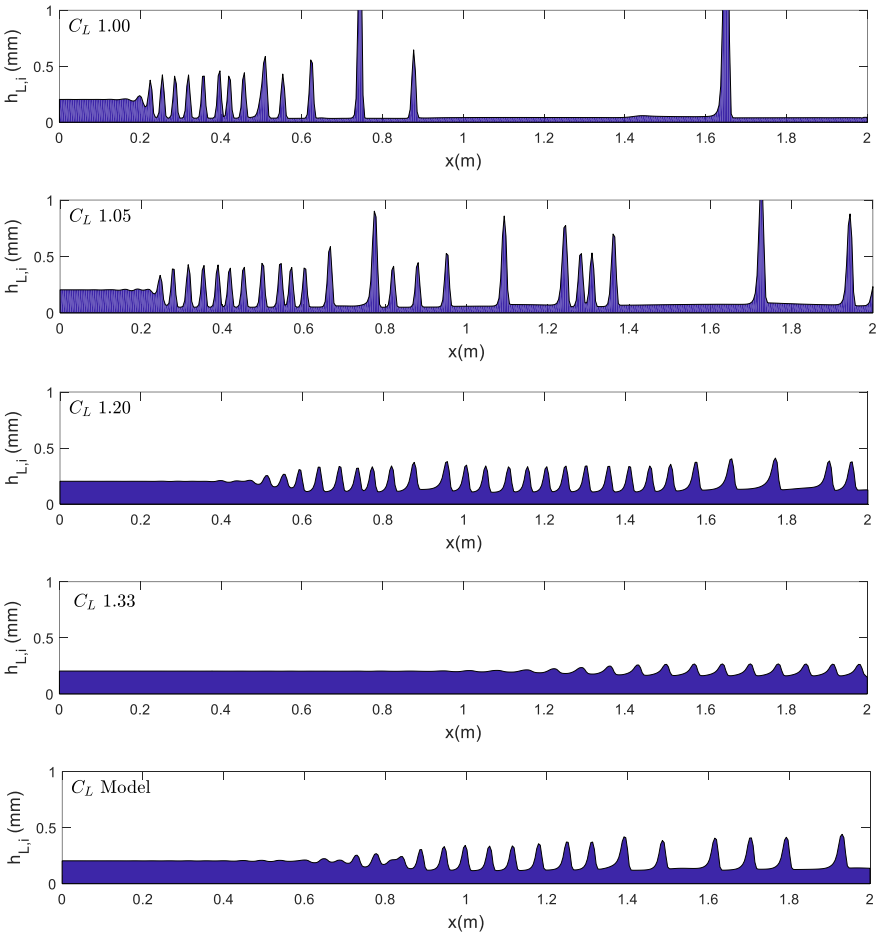

Figure 6. Spatial evolution of the liquid film thickness with different momentum flux parameters. Case II-Zhao.

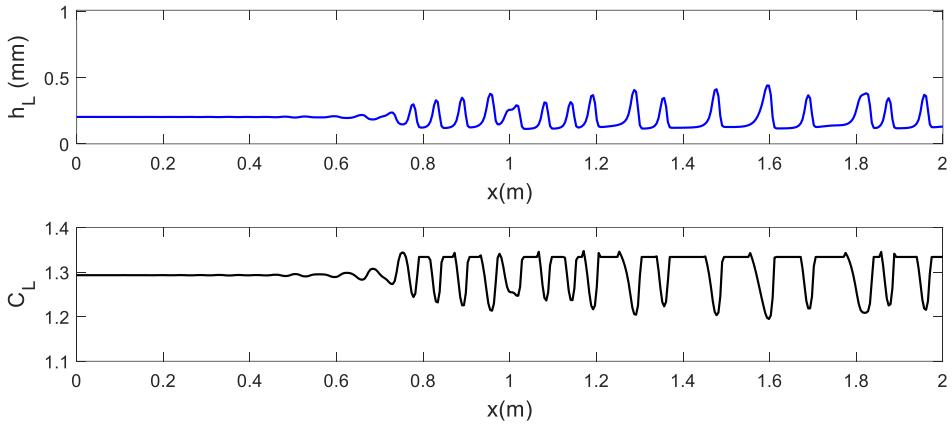

Figure 7. Spatial evolution of the liquid film thickness and C_L. Case II-Zhao.

4. CONCLUSION

The present work evaluated the hydrodynamic stability properties of commonly employed dynamic pressure models and liquid momentum flux parameter values for vertical annular flows with the 1D Two-Fluid Model, as well as proposing and evaluating a novel approach for C_L. Differential and discrete stability analyses were carried out to evaluate the mathematical and discretized version of the system of equations. The closure relations were evaluated through their differential and discrete growth rate curves in the frequency spectrum. Mesh refinements of $\Delta x \ / \ D$= 1 to 0.015625 were selected to generate the discrete dispersion relation curves. The stability analysis results showed that all models provided some measure of stability to the flow and worked to ensure the hyperbolicity of the system of equations. The dynamic pressure models had a small effect in guaranteeing the system's well-posedness, however, it was shown that increasing the empirical constant had significant effects on instability damping. The momentum flux parameter values above 1.05 were able to guarantee the well-posedness of the system, and C_L 1.33 was shown to over-stabilize the wave formation. The proposed C_L model showed very good stability properties and a more physically accurate non-linear effect, and thus has proved to be a promising tool in one-dimensional modelling of pipe flows.

5. ACKNOWLEDGEMENTS

The authors thank the Brazilian Government agencies CAPES and CNPq for the continuous support during the development of this research.

6. REFERENCES

Aliyu, A.M., Baba, Y.D., Liao, L., Yeung, H., Kim, K.C., 2017. Interfacial friction in upward annular gas–liquid two-phase flow in pipes. *Experimental Thermal and Fluid Science*, Vol. 84, pp. 90-109.

Barnea, D. Taitel, Y., 1993. "Kelvin-Helmholtz stability criteria for stratified flow: viscous versus non-viscous (inviscid) approaches". *International Journal of Multiphase Flow*, Vol. 19, No. 4, pp. 639–649.

Belt, R.J., Van't Westende, J.M.C., Portela, L.M., 2009. "Prediction of the interfacial shear-stress in vertical annular flow". *International Journal of Multiphase Flow*, Vol. 35, pp. 689–697.

Bestion, D., 1990. "The physical closure laws in the CATHARE code". *Nuclear Engineering and Design*, Vol. 124, No. 3, pp. 229-245.

Castello Branco, R.L., Carneiro, Fontalvo, E.M.G., J.N.E., de Paula, I.B., Nieckele, A.O., 2022. "Stability analysis of vertical annular flows with the 1D Two–Fluid Model: effect of closure relations on wave characteristics". *International Journal of Multiphase Flow*, Vol. 152, pp. 103947.

Dobran, F., 1983. Hydrodynamic and heat transfer analysis of two-phase annular flow with a new liquid film model of turbulence. *International Journal of Heat and Mass Transfer*, Vol. 26, No. 8, pp. 1159-1171

Fontalvo, E.M.G., Castello Branco, R.L., Carneiro, J.N.E., Nieckele, A.O., 2020. "Assessment of closure relations on the numerical predictions of vertical annular flows with the Two–Fluid Model". *International Journal of Multiphase Flow*, Vol. 126, 103243.

Fowler, A.; Lisseter, P., 1992. "Flooding and flow reversal in annular two-phase flows". *SIAM Journal Applied Mathematics*, Vol. 52, No. 1, pp. 15–33.

Fullmer, W.D., V. H., Ransom, Bertodano, M. A. L., 2014. “Linear and nonlinear analysis of an unstable, but well-posed, one-dimensional Two–Fluid Model for two-phase flow based on the inviscid Kelvin–Helmholtz instability”. *Nuclear Enginnering and Design*, Vol. 268, pp. 173–184. .

Galleni, F., Issa, R.I., 2015. “Linear stability analysis of the discretized one–dimensional Two–Fluid Model equations for slug capturing in vertical flow”. *Multiphase Science Technology*, Vol. 27, No. 2–4, pp. 215–227.

Inada, F., Drew, D. A., & Lahey Jr, R. T., 2004. “An analytical study on interfacial wave structure between the liquid film and gas core in a vertical tube”. *International Journal of Multiphase Flow*, Vol. 30, No. 7-8, pp. 827-851.

Ishii, M., Hibiki, T., 2011. Thermo-Fluid Dynamics of Two Phase Flow, Springer Sc.

Kaji, R., 2008. *Characteristics of two-phase flow structures and transitions in vertical upward flow*. Ph.D. Thesis, University of Nottingham.

Kosky, P. G.; Staub, F. W., 1971. “Local condensing heat transfer coefficients in the annular flow regime”, *AIChe Journal*, Vol. 17, No. 5, pp. 1037-43.

Kushnir, R.; Segal, V.; Ullmann, A.; Brauner, N., 2017. “Closure relations effects on the prediction of the stratified two-phase flow stability via the two-fluid model”. *International Journal of Multiphase Flow*, Vol. 97, pp. 78–93.

Liao, J., Mei, R., Klausner, J.F., 2008. “A study on the numerical stability of the two-fluid model near ill-posedness”. *International Journal of Multiphase Flow*, Vol. 34, pp.1067–1087.

Nieckele, A.O., Carneiro, J.N.E., 2017. “On the numerical modeling of slug and intermittent flows in oil and gas production”. In *Proceedings of ASME 2017 36th Int. Conf. Ocean, Offshore and Arctic Engineering. OMAE2017*. Trondheim, Norway.

Rodriguez, H.T., Soedarmo, A., Pereyra, E., Sarica, C., 2020. Droplet entrainment measurements under high-pressure two-phase low-liquid loading flow in slightly inclined pipes. *Journal of Petroleum Science and Engineering,* Vol. 187, 106767.

Song, J.H.; Ishii, M., 2000. “The well-posedness of incompressible one-dimensional two-fluid model *Nuclear Engineering and Design,* Vol. 43, pp. 2221-2231.

Wallis, G. B., 1969. *One-dimensional two-phase flow*. McGraw-Hill.

Wang, L., Liu, S., Hou, L., Yang. M., Zhang, J., Xu, J., 2022. “Prediction of the liquid film reversal of annular flow in vertical and inclined pipes”. *International Journal of Multiphase Flow*, Vol. 146, 103583.

Whalley, P.; Hewitt, G. F., 1978. “The correlation of liquid entrainment fraction and entrainment rate in annular two-phase flow”. *UKAEA Atomic Energy Research Establishment*.

Versteeg, H.K., Malalasekera, W., 2007. *An Introduction to Computational Fluid Dynamics The Finite Volume Method*, Prentice Hall, 2nd Edition.

Zhao, Y.; Markides, C. N.; Matar, O. K.; Hewitt, G. F., 2013. Disturbance wave development in two-phase gas-liquid upwards vertical annular flow. *International Journal of Multiphase Flow*, Vol. 55, pp. 111-129.

7. RESPONSIBILITY NOTICE

The authors are the only responsible for the printed material included in this paper.